BMC Neuroscience

BioMed Central

Research article

Open Access

Distribution and densitometry mapping of L1-CAM Immunoreactivity in the adult mouse brain – light microscopic observation

Hana Munakata[1], Yukiko Nakamura[1], Kazumasa Matsumoto-Miyai, Kouichi Itoh[2], Hironobu Yamasaki[1] and Sadao Shiosaka*[1]

Address: [1]Division of Structural Cell Biology, Nara Institute of Science and Technology, NAIST, 8916-5 Takayama, Ikoma city, Nara 630-0192, Japan and [2]Tokyo Metropolitan Institute of Medical Science, Tokyo Metropolitan Research Organization, 3-18-22 Honkomagome, Bunkyo-ku, Tokyo 113-8613, Japan

Email: Hana Munakata - munktahn@banyu.co.jp; Yukiko Nakamura - y-nakamu@bs.aist-nara.ac.jp; Kazumasa Matsumoto-Miyai - kmatsumo@bs.aist-nara.ac.jp; Kouichi Itoh - itoh@rinshoken.or.jp; Hironobu Yamasaki - h-yamasa@bs.aist-nara.ac.jp; Sadao Shiosaka* - sshiosak@bs.aist-nara.ac.jp

* Corresponding author †Equal contributors

Published: 16 April 2003

BMC Neuroscience 2003, **4**:7

Received: 26 December 2002
Accepted: 16 April 2003

This article is available from: http://www.biomedcentral.com/1471-2202/4/7

Abstract

Background: The importance of L1 expression in the matured brain is suggested by physiological and behavioral studies showing that L1 is related to hippocampal plasticity and fear conditioning. The distribution of L1 in mouse brain might provide a basis for understanding its role in the brain.

Results: We examined the overall distribution of L1 in the adult mouse brain by immunohistochemistry using two polyclonal antibodies against different epitopes for L1. Immunoreactive L1 was widely but unevenly distributed from the olfactory bulb to the upper cervical cord. The accumulation of immunoreactive L1 was greatest in a non-neuronal element of the major fibre bundles, *i.e.* the lateral olfactory tract, olfactory and temporal limb of the anterior commissure, corpus callosum, stria terminalis, globus pallidus, fornix, mammillothalamic tract, solitary tract, and spinal tract of the trigeminal nerve. High to highest levels of non-neuronal and neuronal L1 were found in the grey matter; *i.e.* the piriform and entorhinal cortices, hypothalamus, reticular part of the substantia nigra, periaqueductal grey, trigeminal spinal nucleus etc. High to moderate density of neuronal L1 was found in the olfactory bulb, layer V of the cerebral cortex, amygdala, pontine grey, superior colliculi, cerebellar cortex, solitary tract nucleus etc. Only low to lowest levels of neuronal L1 were found in the hippocampus, grey matter in the caudate-putamen, thalamus, cerebellar nuclei etc.

Conclusion: L1 is widely and unevenly distributed in the matured mouse brain, where immunoreactivity was present not only in neuronal elements; axons, synapses and cell soma, but also in non-neuronal elements.

Background

L1CAM (L1) is a neural cell adhesion molecule belonging to the immunoglobulin superfamily [1]. In the central nervous system (CNS), L1 is expressed in the developing olfactory bulb, cerebellum and spinal cord [2–9]. In the adult brain, substantial immunoreactive L1 is detected by

western blot and immunohistochemical analyses in the olfactory bulb, cerebellum, cerebral cortex, hippocampus, hypothalamus and spinal cord [5,9–11]. Physiological study has suggested the importance of L1 in the mature brain; *i.e.* neural L1 is involved in Schaffer-collateral long term potentiation (LTP), because it is interfered with on the application of L1-specific antibodies and recombinant L1 fragments [12]. Behavioral analysis has shown that contextual fear conditioning induced L1 expression in the hippocampus [13]. The distribution pattern of L1 might provide a basis for understanding its roles in LTP, fear conditioning, and other unknown functions in the brain. For this reason, we studied the total distribution of L1 in the adult mouse CNS using specific polyclonal antisera against full-length L1 and the C-terminal cytoplasmic domain of L1 at the light microscopic level. Here, we identified novel sites of L1 immunoreactivity in various regions of the brain.

Results

Characterization of antibodies

The specificity of antibodies was checked by both western blotting and immunohistochemistry.

Western blotting

The specificity of antibodies was checked by western blot analysis of the neuropil fractions obtained from mouse hippocampus (Fig. 1a, lanes 1, 2), L1-transfected cell lysate (Fig. 1a, lane 3), and mock-transfected cell lysate (Fig. 1a, lane 4) using anti full-length L1 (antiFLL1; lane 1) and anti C-terminal L1 (antiCTL1; lanes 2–4) antibodies. The antiFLL1 antibody, whose specificity was well-established in another study [2], recognized three bands in the neuropil fraction; the 200-kDa full-length L1, and the 140-kDa N-terminal and 80-kDa C-terminal fragments of L1 (Fig. 1a, lane 1). The antiCTL1 antibody detected two bands; 200-kDa and 80-kDa proteins corresponding to the full-length L1 and its C-terminal fragment, respectively (Fig. 1a, lane 2). To check the specificity of the antiCTL1 antibody further, we blotted High5 cell lysate in which a recombinant rat full-length L1 gene was transfected (Fig. 1a, lane 3) and its control, mock-transfected cell lysate (Fig. 1a, lane 4). A clear single 200 kDa band was seen in L1-transfected cell lysate, but not mock-transfected cell lysate using the antiCTL1 antibody. Thus, both antibodies are highly specific to the L1 protein.

Immunohistochemical characterizations

The two polyclonal antisera (antiCTL1 and antiFLL1 antibodies) demonstrated an analogous staining pattern on immunohistochemistry, though the latter antiserum tended to stain passing proximal axons better than the former (Fig. 6e, insert). Consequently, described here are the results obtained with the antiCTL1 antibody unless specified otherwise. The specificity of immunostaining was checked by three procedures, (1) omission of primary antibodies, (2) absorption of primary antibody (antiCTL1) by cell membrane transfected with the rat full-length L1 gene, and (3) blocking of primary antibody by epidermal growth factor, because it shows a very similar immunohistological distribution profile [14]. No positive structure was found in any of the brain sections of controls (1; Fig. 1b) and (2; 1d',1e',1f'). In contrast, antiCTL1 antibody absorbed with mock-transfected cell membrane or blocked by epidermal growth factor stained positive structures as did antiCTL1 and antiFLL1 antibodies (Fig. 1c,1d,1e,1f). Thus, we concluded that both antibodies are specific.

Three kinds of L1 Immunoreactive structures observed by light microscope

L1 immunoreactive structures were categorized as three kinds of staining profiles under light microscopic observation; *i.e. fibres*, *fine granules and thin fibres*, and *soma*. The immunoreactivity of fibres was generally strong and this type of staining was observed chiefly in the major fibre bundles. In addition, this type of immunostaining was also found in grey matter such as for caudate putamen, hypothalamus, substantia nigra etc. as scattered fibrous immunoreactivity. The staining was observed exclusively in the myelinated tissues, which were composed of at least axons, myelin, oligodendrocytes and astrocytes. To examine whether the immunoreactive L1 is present in the axon itself or non-axonal tissue surrounding the axon, stria terminalis, an amygdalofugal nerve bundle, was cut with knife at the level shown in Figure 3g. The aim of this experiment is to observe whether L1 immunoreactive protein accumulates at the transected axons. If L1 protein accumulates on the side proximal to the amygdala in the transected nerve, this protein certainly travels by axonal flow, and therefore the immunoreactivity in the distal terminal area should be markedly reduced. Since substance P is known to travel in an axonal flow as a neuropeptide [15], L1 protein and substance P should be distributed in a similar manner. After 3 days, the animals were sacrificed and tissue sections were prepared. It was found that there was no accumulation of L1 on the proximal side of the transected nerve (Fig. 2a,2a'), and no reduction of L1 on the distal side of the lesion (Fig. 2c,2c') or in the terminal field (data not shown). In contrast, immunoreactivity for substance P, which is known to be present inside the axons, was accumulated on the proximal side of the transected stria terminalis (Fig. 2b,2b') and also clearly diminished on the distal side of the lesion (Fig. 2d,2d', open arrowheads). This result strongly suggested that L1 in the stria terminalis is not present inside of axons but instead in the myelin, oligodendroglia, or astroglia. Therefore, we described the structures as immunoreactive *fibres* in the present study.

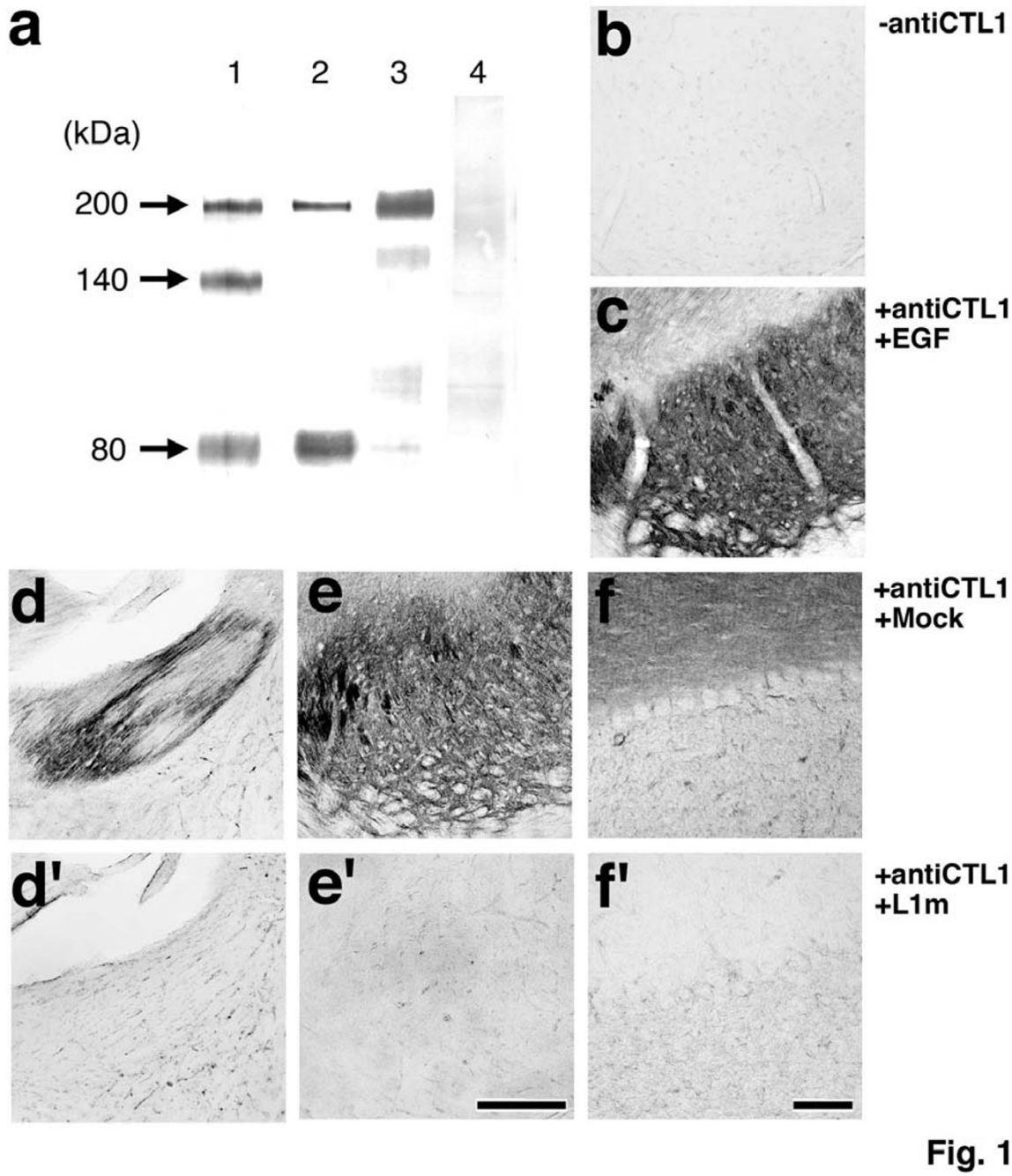

Figure 1

Characterization of antibodies by western blotting, absorption testing and blocking with epidermal growth factor. a. The neuropil fraction (see Materials and Methods) obtained from mouse hippocampus (lanes 1, 2), the L1-transfected cell lysate (lane 3), and the mock-transfected cell lysate (lane 4) were western blotted using the antiFLL1 (lane 1) and antiCTL1 (lanes 2–4) antibodies. AntiCTL1 antibody could detect the full-length (200-kDa) recombinant L1 in the lysate of transfected High5 insect cells (lane 3), whereas no positive band was detectable in the mock-transfected (control) High5 lysate (lane 4). b. Omission of primary antibody (-antiCTL1) resulted in no immunostaining (substantia nigra). c. Blocking of antiCTL1 antibody with epidermal growth factor (EGF) did not interfere with the immunostaining in the neighboring section of (b). d-f,d'-f'. Absorption of the antibody with L1 gene-transfected membrane (L1m) completely eliminated the immunostaining, whereas absorption of the antibody with mock-transfected membrane (Mock) had no effect (d'-f'). d,d': stria terminalis; e,e': substantia nigra; f,f': cerebellar cortex. b-e,d',e': Bar= 200 μm; f,f': Bar = 50 μm.

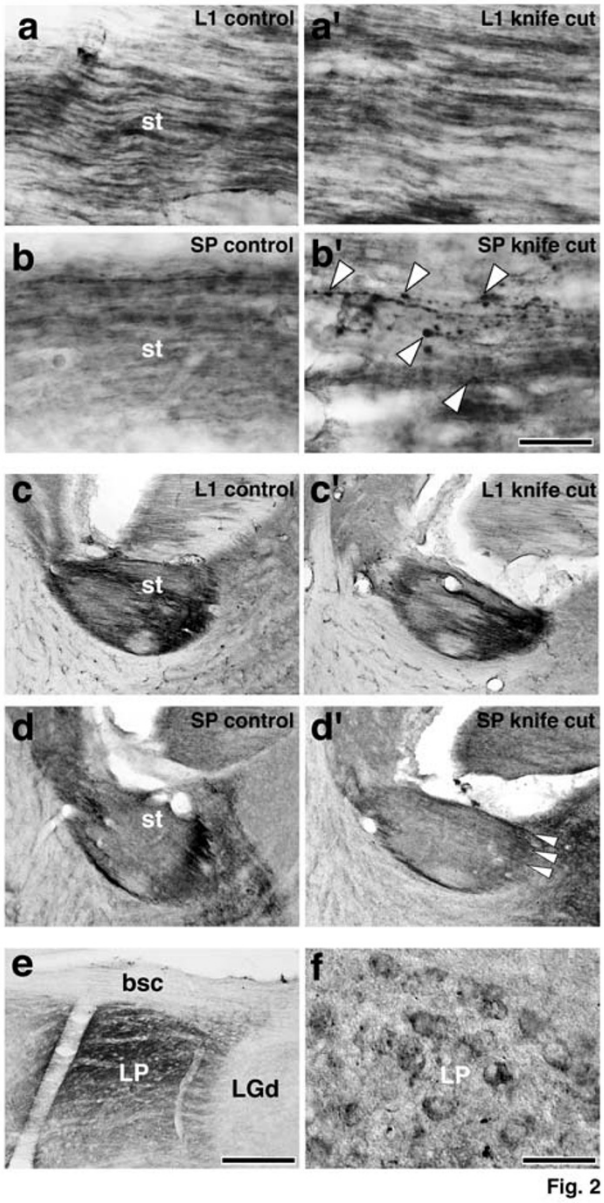

Figure 2

L1 immunoreactive neurons and transection of stria terminalis. a,a' and b,b'. Transection of the stria terminalis resulted in no accumulation of L1 on the proximal side of the nerve (a'; L1 knife cut), but caused accumulation in the case of substance P axons (b', SP knife cut, open arrowheads). L1 control; control side of the same section immunostained with antiCTL1 antibody. SP control; control side of the same section immunostained with antiSP antibody. c,c' and d,d' No change was found on L1 in the distal side of the lesion of the bundle (c'; L1 knife cut), though substance P immunoreactivity was clearly diminished (d'; SP knife cut, open arrowheads). e and f, Bright-field photomicrograph showing L1 neurons in the lateral posterior thalamic nucleus of the upper brainstem. a,a',b,b': Bar = 25 μm; c,c',d,d',e: Bar = 200 μm; f: Bar = 50 μm.

Fine granules and thin fibres with immunoreactivity were exclusively localized to the neuropils in the grey matter. To examine the fine structure more precisely, selected areas with this type of staining were chosen and subjected to an immuno-electron microscopic procedure. We succeeded in demonstrating that they were present in axon terminals or synaptic boutons (Nakamura, Matsumoto-Miyai, and Shiosaka, manuscript in preparation).

The third kind was somatic staining of L1 and this was very rare. There were immunoreactive *soma* in the lateral posterior thalamic nucleus (Fig. 2e,2f).

Densitometry mapping – General features of the L1 immunoreactive structures

L1 immunoreactive structures were distributed unevenly from the olfactory bulb to the upper cervical spinal cord. L1 structures are shown by pseudocolors in the order of highest to lowest density (red, yellow, green, light blue, and blue), with dark blue indicating no L1 (Figs 3 and 4). The highest density of L1 fibres (shown in red) was found in the major anatomical pathways; *i.e.*, the lateral olfactory tract, corpus callosum, stria terminalis, olfactory and temporal limbs of the anterior commissure, globus pallidus, fornix, mammillothalamic tract, solitary tract, and trigeminal spinal tract. Meanwhile, the cortico-spinal pathway (internal capsule, cerebral peduncle, cortico-spinal tract in the midbrain, and pyramid in the medulla oblongata and spinal cord), white matter of cerebellum, cerebellar peduncles, lateral lemniscus, auditory nerve, and white columns of the spinal cord had the lowest density of fibres (blue) or no L1 (dark blue).

The highest density (red) of immunoreactive fine granules in the grey matter of the CNS was found in the bed nucleus of the stria terminalis, preoptic and posterior hypothalamus, piriform to the entorhinal cortex, lateral posterior nucleus of the thalamus, substantia nigra reticular part, periaqueductal grey, caudal reticular nucleus of pons, solitary tract nucleus, and spinal nucleus of the trigeminal nerve. The L1 immunoreactive structure of the spinal nucleus of the trigeminal nerve was concentrated only in the marginal zone and this continued caudally to the substantia gelatinosa of the dorsal horn.

A moderate to low density of immunoreactive fine granules (green to light blue) was found in the granular layer of the olfactory bulb, layer V of the cerebral cortex, cingulate cortex, hypothalamus, amygdala, pontine grey matter, ventral tegmental area of the midbrain, superior colliculi, reticular formation of pons, cerebellar cortex, and parabrachial nucleus. A low to lowest density (light blue to blue) of immunoreactive fine granules was found in the cerebral cortex except for layer V, the caudate-putamen, and the hippocampal formation. In the

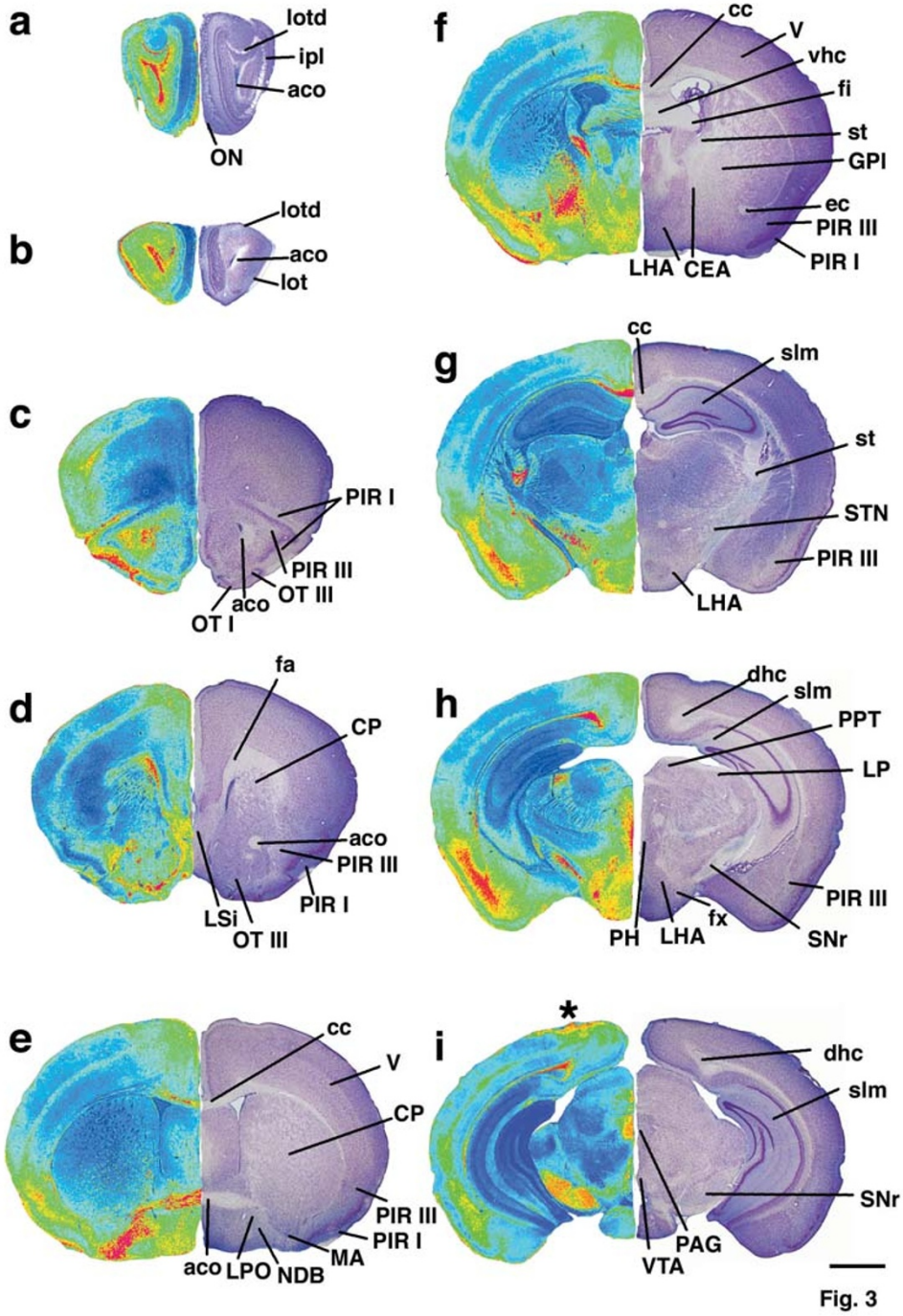

Figure 3

Pseudocolor images of L1 immunoreactive structures in the forebrain and upper brainstem Pseudocolors were as shown in Fig. 4. The cytoarchitecture in the same areas of neighboring sections is presented on the right side as mirror images (a-i). The asterisk that appears in (i) shows a false positive that occurred in areas damaged by tissue processing. Abbreviations are given in the list of abbreviations used. Bar = 1 mm.

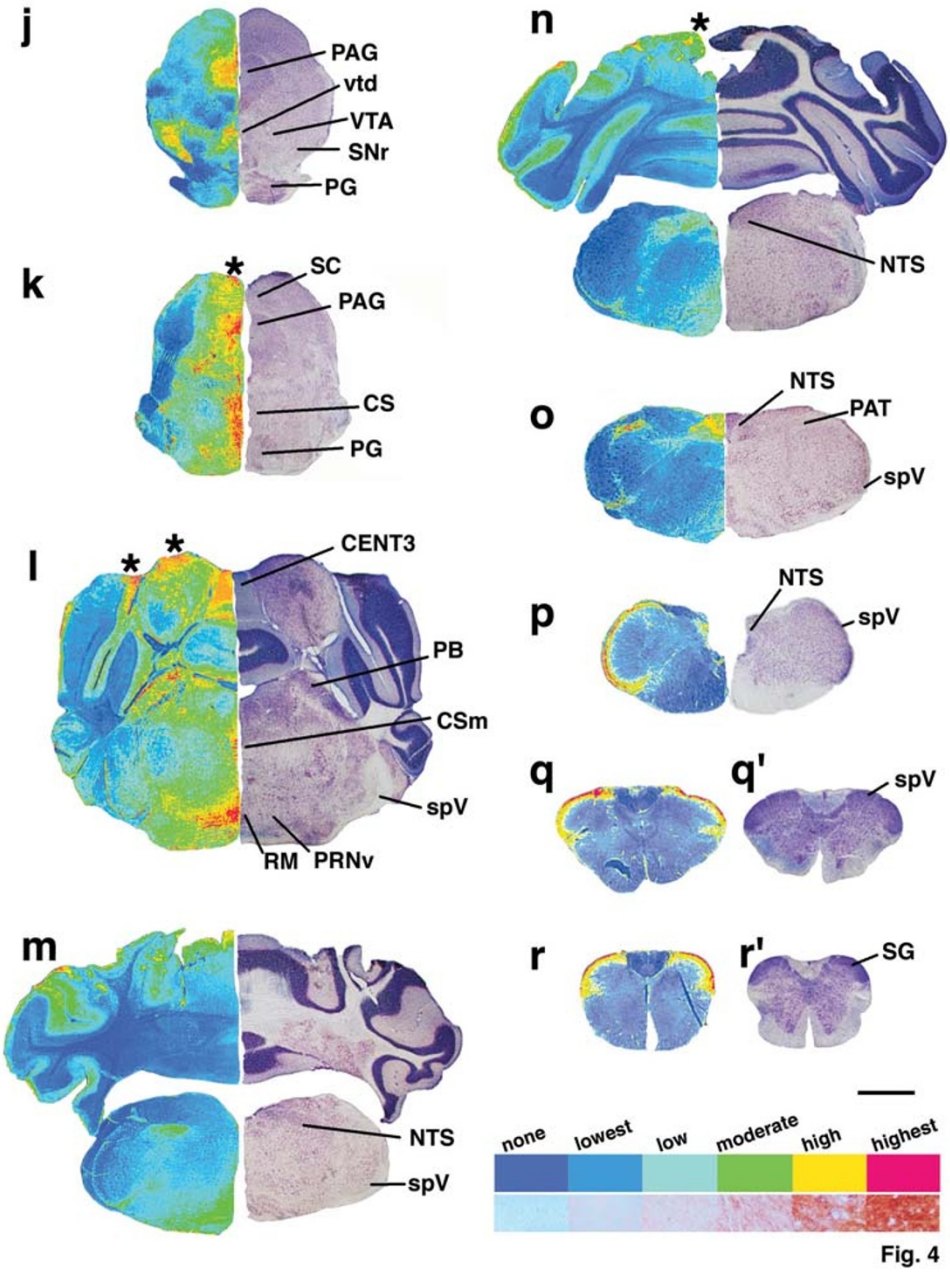

Fig. 4

Figure 4

Pseudocolor images of L1 immunoreactive structures in the cerebellum, lower brainstem and upper cervical spinal cord. Pseudocolors were designated as red (highest), yellow (high), green (moderate), light blue (low), blue (lowest), and dark blue (none) in order of the density of brown oxidized DAB product. The real L1 densities of each pseudocolor were presented (right bottom). The cytoarchitecture in the same areas of neighboring sections is presented on the right side as mirror images (j-p q, q', r, r'). The asterisks show a false positive caused by damaged tissue. Bar = 1 mm.

hippocampal formation, stratum lacunosum moleculare and CA3 had a low level (light blue) of L1, though other areas of Ammon's horn and the dentate gyrus showed only very faint (blue) or no (dark blue) immunoreactivity. In the cerebellum, the molecular layer of all lobes had moderate immunoreactivity (green) as shown above, whereas the granular layer had the lowest level (blue) of L1 (Fig. 4l,4m,4n). In total, L1 was concentrated in brain in a site-specific manner where the limbic, gustatory and somatosensory nervous systems are located.

L1 immunoreactive structures in the forebrain

Olfactory bulb

The highest density of L1 immunoreactive fibres was found in the olfactory nerve, the primary nerve from the olfactory receptor, though there was only faint immunoreactivity in the olfactory glomeruli (Figs. 3,5a,5b). The density of L1 immunoreactive fibres was also highest in the lateral olfactory tract and its dorsal limb (Fig. 5a, insert), and in the anterior commissure, olfactory limb (Fig. 5a). A moderate density of immunoreactive fine granules was observed both in the internal plexiform layer and granular cell layer (Fig. 5a,5b). However, no immunoreactivity was found in the mitral cell layer.

Cerebral cortex

The piriform and entorhinal cortex, which are terminal fields of the olfactory pathway, had the highest density of immunoreactive fine granules among all cortical areas (Figs. 3c,3d,3e,3f,3g,3h,3i,5e,5f). The immunoreactivity was spread over layer I and III in the piriform area, and layer I and III-V in the entorhinal area, though only a low density of immunoreactive granules was found in layer II of both cortical areas. The cingulate area had the next densest accumulation of L1 immunoreactive granules among the cortical areas. However, the lowest density of L1 immunoreactive fine granules was found in the neocortex, as shown in the densitometry map, except for layer V which had a moderate density of immunoreactivity (Figs. 3, 5d).

Caudate-putamen, internal capsule and globus pallidus

The mouse caudate-putamen contained fibre bundles appearing as uniformly scattered spots in coronal sections. The bundles contained a few, strong immunoreactive fibres in the dorsolateral portion, and more immunoreactive fibres in the ventromedial portion (Figs. 3, 5g,5h). On the other hand, grey matter of the caudate-putamen had the lowest density of immunoreactive fine granules (Fig 5g,5h). The globus pallidus had the highest density of L1 immunoreactive fibres (Fig. 5i,5j). In contrast, thick bundles of the internal capsule, cerebral peduncle and the pyramid lacked immunoreactive fibres (Figs. 3f,4j,4k,4l,4m,4n,4o,5i,6c,7d,7h).

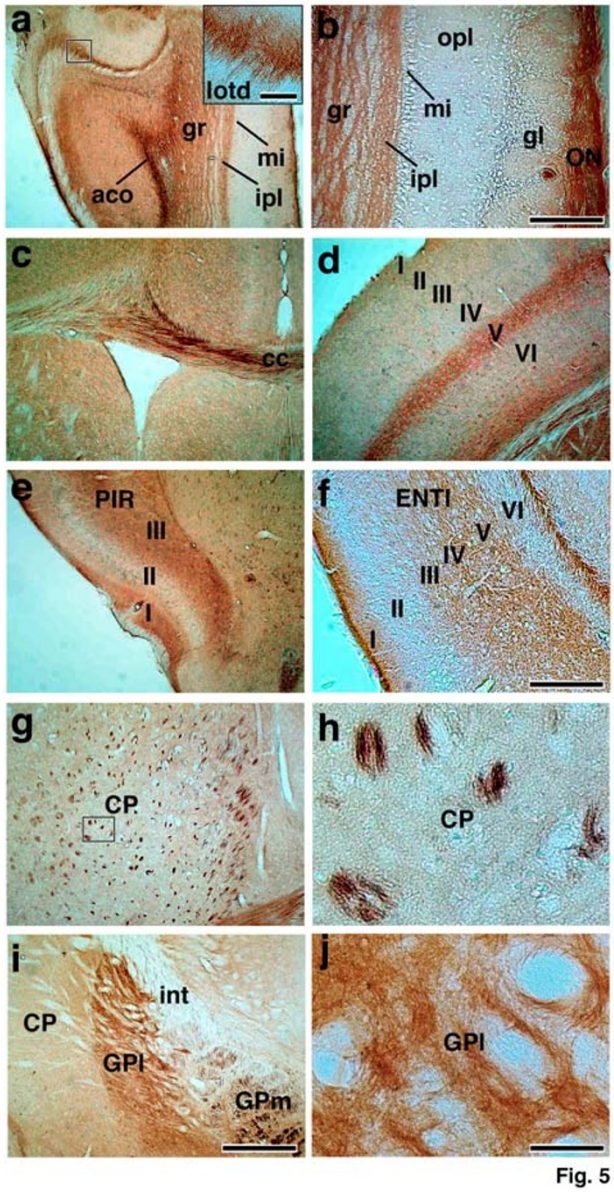

Fig. 5

Figure 5

L1 immunoreactive structures in the forebrain. a-j, Bright-field photomicrographs showing L1 structures in the olfactory bulb (a and b), corpus callosum (c), cerebral cortex (d), piriform cortex (e), entorhinal cortex (f), caudate putamen (g and h), and globus pallidus (i and j). A magnified view of the square in (a) is shown in the insert. b, h, and j represent higher magnification photomicrographs of the olfactory bulb, caudate putamen, and globus pallidus. a,c-f: Bar = 250 μm; insert in a: Bar = 50 μm; b: Bar = 200 μm; g,i: Bar = 500 μm; h,j: Bar = 50 μm.

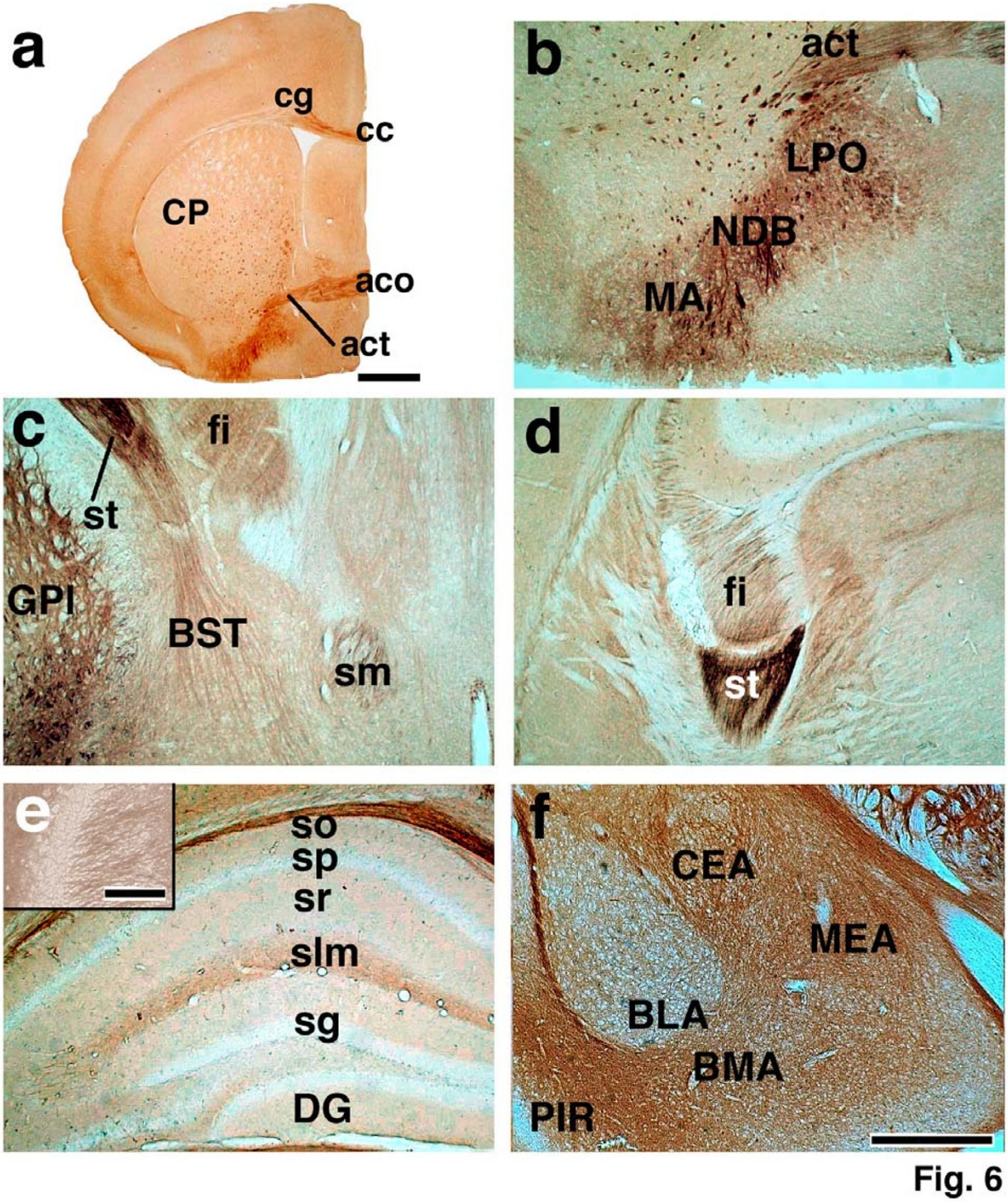

Figure 6

L1 immunoreactive structures in the limbic areas. a-f. Bright-field photomicrographs showing the preoptic area of the hypothalamus (a and b), bed nucleus of stria terminalis (c), stria terminalis (c and d), hippocampus (e), and amygdaloid complex (f). A higher magnification photograph of CA3 which was immunoreacted with antiFLL1 antibody is shown in the insert in (e). Note that better staining for proximal axons was found in CA3 than with antiCTL1 antibody. a: Bar = 1 mm; b-f: Bar = 500 μm; insert in e: Bar = 100 μm.

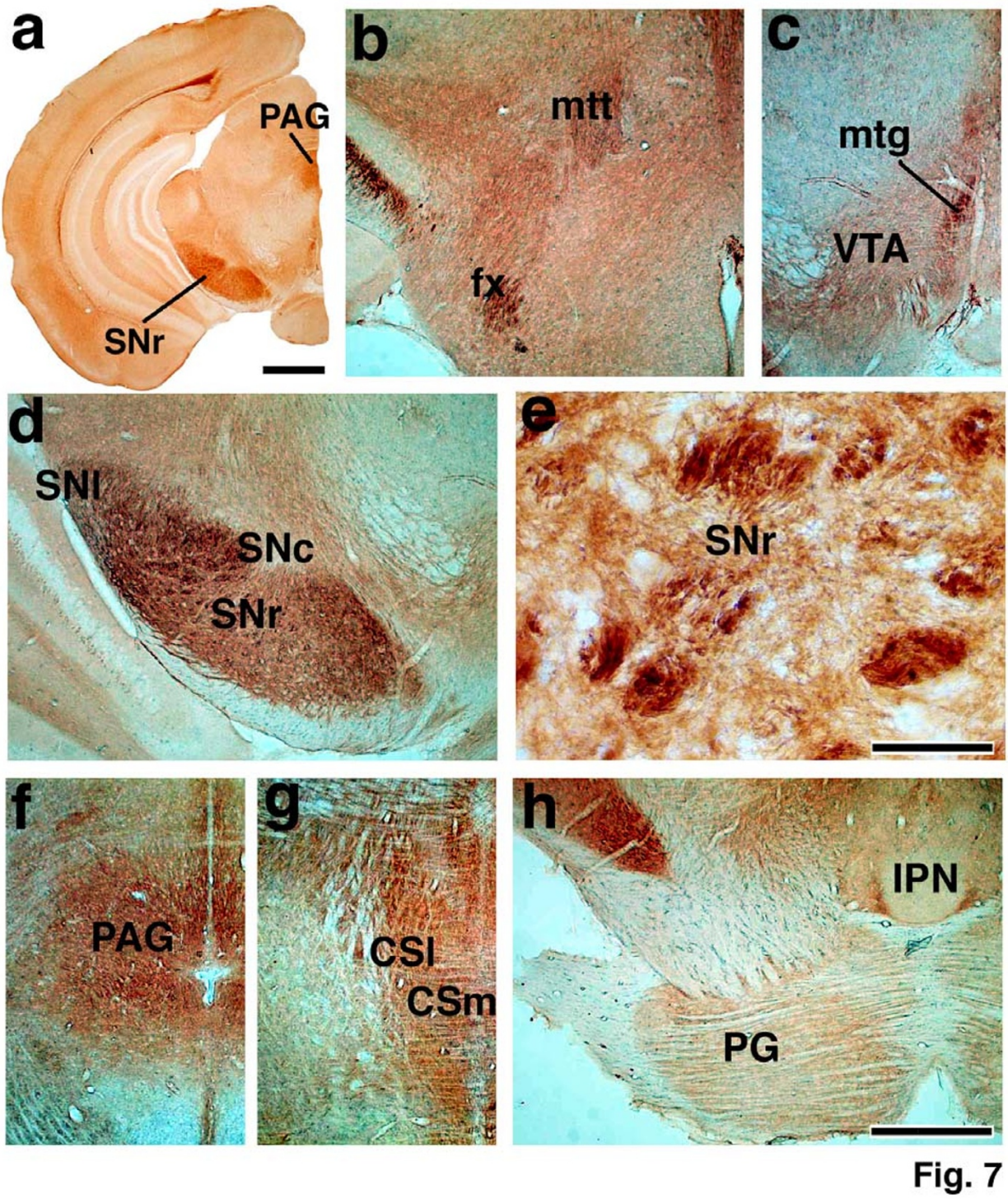

Figure 7

L1 immunoreactive structures in the posterior hypothalamus, midbrain, and pons. a-h. Bright-field photomicrographs showing low power micrographs of the midbrain (a), posterior hypothalamus (b), ventral tegmental area (c), and reticulate part of substantia nigra (d), and higher magnification photographs of the substantia nigra (e), periaqueductal grey (f), central superior nucleus of the raphe (g), interpeduncular and pontine nucleus (h). a: Bar = 1 mm; b-d,f-h: Bar = 500 μm; e: Bar = 50 μm.

Corpus callosum, and anterior commissure

The corpus callosum and anterior commissure interconnect between two neocortices and two olfactory bulbs, respectively. The bundles contained the highest density of L1 immunoreactive fibres (Figs. 5c,6a,6b).

Stria terminalis, bed nucleus of stria terminalis, and preoptic area

The major amygdalofugal projection to the hypothalamus passes through the stria terminalis. The highest density of L1 immunoreactive fibres was localized in the stria terminalis (Fig. 2a,2a',6c,6d). On the other hand, the bed nucleus of stria terminalis, nucleus of the diagonal band of Broca, lateral hypothalamic preoptic area, and magnocellular preoptic nucleus had a high density of immunoreactive fibres and fine granules (Fig. 3, 6b,6c).

Hippocampus and amygdala

Fimbria had a moderately dense accumulation of immunoreactive fibres (Fig. 6d). A considerable number of L1 immunoreactive fibres were localized in the stratum lacunosum moleculare (Fig. 6e). However, most of the hippocampal formation exhibited the lowest density of immunoreactivity. In the CA3, thin fibres which had arisen from pyramidal cell soma were immunostained when the tissue sections were reacted with antiFLL1 (Fig. 6e, insert). In the stratum radiatum and oriens of the CA1 and CA2 and stratum moleculare of the dentate gyrus, the density of fine L1 immunoreactive fine granules was lowest (Fig. 6e).

In contrast to the hippocampus, the amygdala was rather rich in immunoreactive fine granules at a moderate to low level. A moderate level of fine granules with immunoreactivity was present in the medial and lateral amygdaloid nucleus and less immunoreactivity in the lateral and basal lateral nucleus (Figs. 3,6f).

Thalamus

There were only a few immunoreactive fibres in this nucleus other than in fibre bundles such as the mammillothalamic tract (described below).

Major thalamic areas contained only low to lowest levels of immunoreactive fine granules (Fig. 3). The lateral posterior thalami had the highest density of immunoreactive fine granules (Fig. 2e,2f). This nucleus contained a number of positive neurons, in which cytoplasm was densely immunostained by anti L1 antisera (Fig. 2f).

Hypothalamus

Immunoreactive fibres and fine granules were found with the highest density in the hypothalamic and posterior hypothalamic areas (Figs. 3e,3f,3g,3h,6a,6b,7b). The medial forebrain bundle, which is the major hypothalamic bundle interconnecting the forebrain with the lower brainstem, had numerous immunoreactive fibres and two major bundles pass through the hypothalamus; the fornix and mammillothalamic tract contained strongly immunoreactive fibres (Fig. 7b). Grey matter all over the hypothalamus was rich in immunoreactive fine granules (Figs. 3,6a,6b,7b)

Substantia nigra and ventral tegmental area

A number of immunoreactive fibres were localized in the reticular part of the substantia nigra, particularly in its dorsolateral portion (Figs. 3h,3i,7a,7d,7e). The reticular part of the substantia nigra contained the highest density of immunoreactive fine granules in its ventromedial part. The ventral tegmental area contained a moderate number of immunoreactive fine granules (Fig. 7c). On the other hand, the compact part of this nucleus had only a low level of immunoreactive granules.

L1 immunoreactive structures in cerebellum and lower brainstem

Interpeduncular nucleus, pontine grey matter, and periaqueductal grey matter

Periaqueductal grey had the highest density of immunoreactive fibres (Figs. 4j,4k,7f). The dorsolateral and lateral parts of the interpeduncular nucleus had a moderate level of immunoreactivity, though intermediate, rostral and caudal parts of the nucleus lacked any immunoreactivity (Fig. 7h). Pontine grey matter had a moderate accumulation of fine L1 immunoreactive granules (Figs. 3j,3k,7h). The central superior nucleus of the raphe had the highest density of fine L1 immunoreactive granules (Figs. 3k,7g).

Cerebellum

The white matter and three cerebellar peduncles lacked immunoreactive fibres (Fig. 4k,4l,4m,4n). The molecular layer of the cerebellar cortex had a moderate level of immunoreactive fine granules in all lobes of the cerebellum as shown in the densitometry map (Fig. 4l,4m,4n). The staining was homogenous and fine (Fig. 8a,8b,8c). The Purkinje cells were not immunostained. In the inner granular layer, lowest level of immunoreactive granules was found. Deep cerebellar nuclei had the lowest density of immunoreactive fine granules.

Solitary tract, solitary tract nucleus and area postrema

A moderate number of L1 immunoreactive fibres was found in the solitary tract (Fig. 8d,8e). The nerve ran dorsomedially in the medulla oblongata and entered the solitary tract nucleus (Figs. 4m,4n,4o,4p, 8d,8e). The density of immunoreactive granules was greatest here with a less dense accumulation extending to the nucleus prepositus (Fig. 8d,8e). The area postrema had a moderate density of immunoreactive fibres (Fig. 8e).

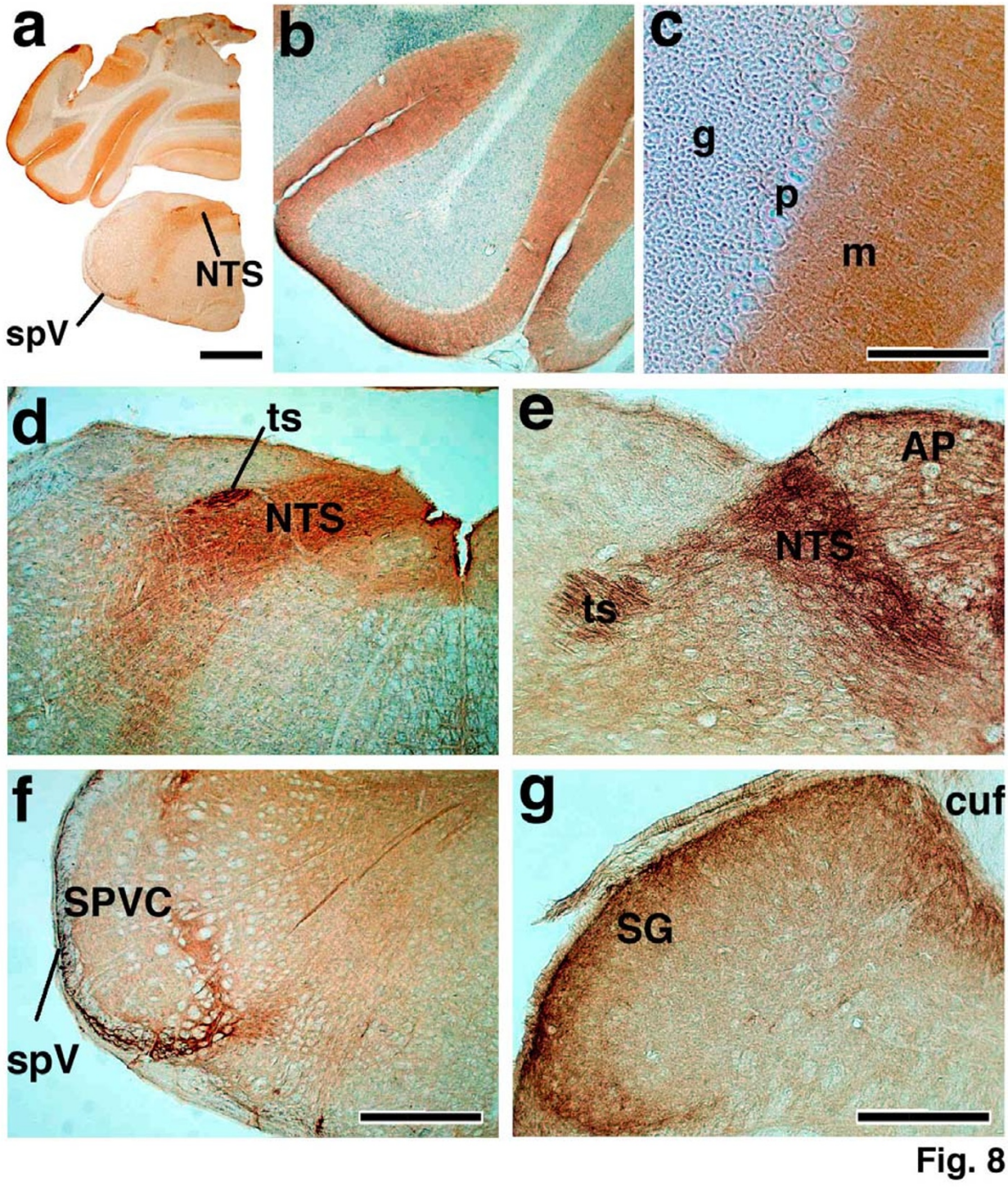

Figure 8

L1 immunoreactive structures in the cerebellum, lower brainstem, and upper cervical spinal cord. a-g. Bright-field photomicrographs showing low power micrographs of the cerebellum and lower brainstem (a), and cerebellar cortex (b), and higher magnification photographs of the cerebellar cortex (c), the solitary tract nucleus (d), caudal of photograph d (e), the trigeminal spinal nucleus (f), and the dorsal horn of cervical spinal cord (g). a: Bar = 1 mm; b,d,f: Bar = 500 μm; c: Bar = 100 μm; e,g: Bar = 200 μm.

Trigeminal spinal nucleus and upper cervical cord

The spinal tract of the trigeminal nerve contained the highest density of L1 immunoreactive fibres (Fig. 4o,4p,4q). In the oral part of the spinal nucleus of the trigeminal nerve, immunoreactive fine granules were localized to the deep layer in the ventral-most and dorsal-most parts (Figs. 4o,8f). Caudally, immunoreactive fine granules concentrated in the marginal zone of this nucleus at high density (Fig. 4p,4q,4q'). This localization pattern extended to the superficial dorsal horn, particularly the substantia gelatinosa in a similar manner at the level of the cervical spinal cord (Figs. 4r,4r',8g).

Discussion

The present study has shown a detailed densitometic distribution of L1 immunoreactive structures in the adult mouse brain. The map showed that L1 protein is widespread but unevenly distributed in adult mouse brain. Some previous studies pointed that L1 is expressed in adults in the olfactory bulb [16], optic nerve [17], hippocampus [8,10,11] and cerebellum [18]. We confirmed these findings except for those in the optic nerve and further identified novel sites of expression of L1, which had not been described before. The areas were the piriform and entorhinal cortices, hypothalamus, globus pallidus, amygdala, periaqueductal grey, reticular part of substantia nigra, pontine grey, superior colliculi, solitary tract nucleus, and trigeminal tract nucleus. Such areas are of common neurophysiological significance, *i.e.* the limbic and sensory systems, and therefore, L1 is considered to be closely associated with these systems. In addition, the distribution of L1 in the limbic brain (hippocampus, hypothalamus, and amygdala) as shown in the present study might partly support the involvement of L1 in contextual fear conditioning [13,19] and neural plasticity like hippocampal LTP [12]. However, it is notable that the auditory system (cochlear nucleus, lateral leminiscal pathway, inferior colliculi, and medial geniculate body) had very little or no L1. This might show that L1 does not participate in auditory functions compared to other sensory functions; olfactory, visual (optic nerve) [20], gustatory and somatosensory.

There is some discrepancy between our study and previous studies. It has been believed that non-myelinated axons with L1-immunoreactivity exist in thick fibre bundles [6]. Our study confirmed strong immunostaining in the corpus callosum, and anterior commissure detected light-microscopically. We have newly demonstrated in the present study that the stria terminalis and hypothalamic fibre bundles had similar staining patterns. To examine whether the L1 in the thick bundles is the axon itself or a non-axonal glial component, the stria terminalis was cut to observe whether L1 immunoreactive protein and substance P accumulate at the transected axons (Fig. 2a,2a'). However, there was no accumulation of L1 in transected nerve, and no reduction in the terminal field of the stria terminalis. In contrast, substance P, an anterogradely transported neuropeptide, was densely accumulated at the site of transection and diminished in immunoreactivity on the distal side and in its terminal field, *i.e.* the bed nucleus of the stria terminalis [15]. Therefore, the result did not support the notion that L1 is present in the axons of the thick bundles, though a more detailed study using an electron microscope is necessary (see Fig. 2a,2b,2c,2d).

Hulley et al. has pointed out that L1 might function as a survival factor for dopaminergic neurons in the foetus and adults [21]. L1-positive fine granules which consisted of nerve terminals were concentrated in the reticular part of the substantia nigra and ventral tegmental areas as shown in the present study. L1-positive nerve terminals in the reticular part may possibly associate with dendrites of dopaminergic neurons. If there is direct interaction between L1 immunoreactive nerve terminals and dopaminergic neurons, such dopaminergic neurons might receive survival signals via synaptic connection. More studies are needed to examine such effects; *i.e.* double immunoelectron microscopic analysis to detect L1 and dopamine-related molecules, and a biochemical approach to detect L1 in the dopaminergic signalling system. Similarly, recent analysis indicates that L1 might be involved in axonal elongation and target recognition of injured cholinergic axons in the adult hippocampal formation [22]. The injured cholinergic neurons which are regenerating their axons upregulate L1, and downregulate it upon target innervations. Therefore, L1 might play important roles in elongation, survival, and recognition in a particular subset of the nervous system.

Conclusions

L1 is widely and unevenly distributed in the matured mouse brain, where immunoreactivity was present not only in neuronal elements; axons, synapses and cell soma, but also in non-neuronal elements. Further study will be necessary to reveal the functional significance of L1 in the matured brain.

Methods

Animal and Tissue Processing

Twenty-one 8-week old male C57BL / 6J mice which were purchased from SLC Co. (Hamamatsu, Japan) were maintained under a 12/12 hour light/dark cycle with ad libitum feeding. The mice were anesthetized with an intraperitoneal injection of 10 % ethyl carbamate (10 μl per g body weight). They were then perfused transcardially through the ascending aorta with 100 ml of saline and 100 ml of a fixative containing 4% paraformaldehyde in 0.1 M phosphate-buffered saline (PBS; pH. 7.4) at room temperature. Brains were removed and postfixed over-

night in the same fixative at 4°C and then immersed in 0.1 M phosphate buffer (pH. 7.4) containing 30 % sucrose for cryoprotection at 4°C. Frozen serial sections 30 μm thick were cut on a cryostat at -15°C.

Three male mice (8 weeks old) were used for a knife-cut study of the stria terminalis from the amygdaloid complex to the bed nucleus of the stria terminalis and preoptic hypothalamus. Hemi-transection of the stria terminalis at the bregma -1.7 mm, 3.0 mm lateral and 4.0 mm deep was carried out and the animals survived for 3 days. Tissue sections were produced as described above.

Immunohistochemistry

The tissue sections were incubated in 0.6% H_2O_2 in 0.1 M PBS for 45 min and then in cold PBS containing 1% bovine serum albumin (Sigma type V, St. Louis, MI) for 60 min prior to the start of immunohistochemistry. L1 immunoreactive structures were demonstrated in every third section. The neighboring sections were used for control experiments (controls of L1 absorption and of omission of primary antibody). The sections used for demonstrating L1 structures were incubated in L1 antiserum (1:200 dilution for antiCTL1 and 1:500 for antiFLL1). For detection of antiCTL1, biotinylated anti-goat immunoglobulin G (IgG) secondary antibody was used at 1:1000. For detection of antiFLL1, biotinylated anti-rabbit IgG secondary antibody was used at 1: 1500. After being rinsed with cold PBS, the sections were incubated in avidin-peroxidase complex (ABC kit; Vector Laboratories, Burlingame, CA). Following a rinse in PBS, the sections were immersed in 0.05% 3,3'-diaminobenzidine tetrahydroxychloride (DAB) in 0.05 M Tris-HCl buffer, pH 7.5, containing 0.01% H_2O_2 for 5 min to detect peroxidase. Immunostaining for substance P was described in Sakanaka et al. [15].

Observation was under a Nikon Lab photo 2 microscope equipped with a normal condenser or Zeiss Axioplan 2 differential interference microscope. Digital images of each section were captured through a PDMC IIi digital camera (Polaroid, Tokyo, Japan) and analyzed with Win Roof image analysis software (Mitani Co., Fukui, Japan). Tissue sections for digital images were prepared at the same time under the same conditions to avoid fluctuations in the strength of immunoreactivity among experiments. Pseudocolors were red, yellow, green, light blue, blue, and dark blue in order (high to none) of the density of the brown oxidized DAB product. The sections subjected to Nissl staining after the capture of immunohistological images and the cytoarchitecture are presented on the right side as mirror images.

Primary antibodies

Two antibodies against different epitopes were used as primary antibody for L1 in the present study; one was an affinity-purified goat polyclonal antibody (Santa Cruz Biotechnology Inc., Santa Cruz, CA) raised against the C-terminus synthetic peptide of mouse L1 (antiCTL1) and the other was a rabbit polyclonal antibody for full-length L1 (antiFLL1; provided by Dr. V. Lemmon).

Characterization of primary antibodies

For western blotting, the neuropil preparation was prepared as described previously but with slight modification [23]. Briefly, hippocampi were removed from adult ddY male mice (8 weeks old, Japan SLC) and homogenized in chilled homogenizing buffer (125 mM NaCl, 1 mM potassium acetate, 100 mM sucrose, and 50 mM HEPES pH 7.5) with five turns of a Teflon pestle. The homogenate was filtered sequentially through 3 layers of nylon mesh (100-μm pore size) and a 5 μm Millipore filter. The filtered particulate was then centrifuged at 1000 g for 15 min at 4°C. The pellet (neuropil preparation) was resuspended in 1 ml of lysis buffer (1% Triton X-100, 150 mM NaCl, 5 mM EDTA, and 50 mM HEPES pH 7.4), then this suspension was centrifuged at 15,000 rpm for 30 min in a Microfuge to clear the debris. The supernatant was used for western blotting as described [5].

For histochemical characterization, antiCTL1 antibody was pre-absorbed with L1-transfected cell membrane. The rat L1 cDNA was subcloned into the pVL1392 transfer vector plasmid. Plasmid DNA was transferred into the AcNPV genome by homologous recombination so that Sf9 cells were transfected with the L1 transfer plasmid and AcNPV DNA. To express L1, High5 cells were infected with recombinant baculovirus. Three days post-infection, the L1-transfected High5 cells were harvested, washed, and resuspended in ice-cold hypotonic lysis buffer containing 20 mM HEPES (pH 7.4), 1 mM EDTA, 0.02% sodium azide, and 100 mM phenylmethanesulfonyl fluoride (PMSF). The cell lysate was subsequently sonicated and centrifuged three times at 1000 × g. After each centrifugation, the supernatants were collected and pooled. The membrane fraction was precipitated by centrifugation of the pooled supernatant at 100,000 × g for 1 h. The antiCTL1 antibody (2 μg) was absorbed with the L1-expressing cell membrane fraction (2×10^7 cells) resuspended in 1 ml of 0.1 M PBS, 5 % bovine serum albumin, and 100 mM PMSF at 4°C for 48 h. After the centrifugation at 100,000 × g for 1 h, the supernatant was used as the pre-absorbed L1 antibody. As a control, we prepared antiCTL1 antibody absorbed with the mock-transfected cell membrane fraction. In addition, we prepared blocking antiCTL1 antibody which was pre-incubated with epidermal growth factor (Sigma, St Louis, MO; 10 μ/1 μg of antibody).

Nomenclature

Terminology is based upon the atlases of Sidman, Angevine and Pierce [24] and Hof, Young, Bloom, Belichenko and Celio [25].

Authors' contributions

HM and YN equally contributed to this study. HM and YN carried out tissue dissection, immunohistochemistry, and data analysis. KMY conducted immunohistochemistry, characterization of antibodies, and data analysis. KI produced another L1 antibody that was not presented in the study and conducted data analysis. HY participated in the absorption test of the antibodies. SS conceived this study, conducted its design, and coordination, and wrote the manuscript.

List of Abbreviations used

aco, anterior commissure, olfactory limb; act, anterior commissure, temporal limb; antiCTL1 antibody, anti C-terminal L1 antibody; antiFLL1 antibody, anti full-length L1 antibody; AP, area postrema; BLA, basolateral nucleus of the amygdala, ventral part; BMA, basomedial nucleus of the amygdala; bsc, brachium of the superior colliculus; BST, bed nucleus of the stria terminalis; cc, corpus callosum; CEA, central nucleus of the amygdala; CENT3, central lobe of the cerebellum, lobule 3; cg, cingulum bundle; CNS, central nervous system; CP, caudate-putamen; CS, central superior nucleus of the raphe; CSl, central superior nucleus of the raphe, lateral part; CSm, central superior nucleus of the raphe, medial part; DG, dentate gyrus; dhc, dorsal hippocampal commissure; ec, external capsule; ENTl, entorhinal cortex, lateral part; fa, corpus callosum, anterior forceps; fi, fimbria; fx, fornix; gl, glomerular layer; GPl, globus pallidus, lateral part; GPm, globus pallidus, medial part; gr, granule cell layer; int, internal capsule; ipl, internal plexiform layer; IPN, interpeduncular nucleus; LGd, lateral geniculate nucleus, dorsal part; LHA, lateral hypothalamic area; lot, lateral olfactory tract; lotd, lateral olfactory tract, dorsal limb; LP, lateral posterior nucleus of the thalamus; LPO, lateral preoptic area; Lsi, lateral septum nucleus, intermediate part; MA, magnocellular preoptic nucleus; MEA, medial nucleus of the amygdala; mi, mitral cell layer; mtg, mammillotegmental tract; mtt, mammillothalamic tract; NDB, nucleus of the diagonal band of Broca; NTS, nucleus of the solitary tract; ON, olfactory nerve; opl, outer plexiform layer; OT, olfactory tubercle; PAG, periaqueductal grey matter; PAT, paratrigeminal nucleus; PB, parabrachial nucleus; PG, pontine grey matter; PH, posterior hypothalamic area; PIR, piriform cortex; PPT, posterior pretectal nucleus; PRNv, pontine reticular nucleus, ventral part; RM, nucleus raphe magnus; SC, superior colliculus; SG, substantia gelatinosa; sg, stratum granulosum; slm, stratum lacunosum moleculare; sm, stria medullaris; SNc, substantia nigra, compact part; SNl, substantia nigra, lateral part; SNr, substantia nigra, reticular part; so, stratum oriens; sp, stratum pyramidale; spV, spinal tract of the trigeminal nerve; sr, stratum radiatum; st, stria terminalis; STN, subthalamic nucleus; V, Vth layer of the cerebral cortex; vhc, ventral hippocampal commissure; VTA, ventral tegmental area; vtd, ventral tegmental decussation.

Acknowledgements

Thanks to Dr. V. Lemmon (Case Western Reserve Univ., Cleveland, OH, U.S.A.) for kindly providing anti-full length L1 antibody. SS and KMY are supported by grants (14658251, 14780601) from the Ministry of Science, Sport, Culture and Technology.

References

1. Moos M, Tacke R, Scherer H, Teplow D, Fruh K and Schachner M **Neural adhesion molecule L1 as a member of the immunoglobulin superfamily with binding domains similar to fibronectin** *Nature* 1988, **334:**701-703
2. Lemmon V, Farr KL and Lagenaur C **L1-mediated axon outgrowth occurs via a homophilic binding mechanism** *Neuron* 1989, **2:**1597-1603
3. Ignelzi MA Jr, Miller DR, Soriano P and Maness PF **Impaired neurite outgrowth of src-minus cerebellar neurons on the cell adhesion molecule L1** *Neuron* 1994, **12:**873-884
4. Lindner J, Rathjen FG and Schachner M **L1 mono- and polyclonal antibodies modify cell migration in early postnatal mouse cerebellum** *Nature* 1983, **305:**427-430
5. Liljelund P, Ghosh P and van den Pol AN **Expression of the neural axon adhesion molecule L1 in the developing and adult rat brain** *J Biol Chem* 1994, **269:**32886-32895
6. Joosten EA, Gribnau AA and Gorgels TG **Immunoelectron microscopic localization of cell adhesion molecule L1 in developing rat pyramidal tract** *Neuroscience* 1990, **38:**675-686
7. Persohn E and Schachner M **Immunoelectron microscopic localization of the neural cell adhesion molecules L1 and N-CAM during postnatal development of the mouse cerebellum** *J Cell Biol* 1987, **105:**569-576
8. Persohn E and Schachner M **Immunohistological localization of the neural adhesion molecules L1 and N-CAM in the developing hippocampus of the mouse** *J Neurocytol* 1990, **19:**807-819
9. Miragall F and Dermietzel R **Immunocytochemical localization of cell adhesion molecules in the developing and mature olfactory system** *Microsc Res Tech* 1992, **23:**157-172
10. Miller PD, Chung WW, Lagenaur CF and DeKosky ST **Regional distribution of neural cell adhesion molecule (N-CAM) and L1 in human and rodent hippocampus** *J Comp Neurol* 1993, **327:**341-349
11. Schuster T, Krug M, Stalder M, Hackel N, Gerardy-Schahn R and Schachner M **Immunoelectron microscopic localization of the neural recognition molecules L1, NCAM, and its isoform NCAM180, the NCAM-associated polysialic acid, beta1 integrin and the extracellular matrix molecule tenascin-R in synapses of the adult rat hippocampus** *J Neurobiol* 2001, **49:**142-158
12. Luthl A, Laurent JP, Figurov A, Muller D and Schachner M **Hippocampal long-term potentiation and neural cell adhesion molecules L1 and NCAM** *Nature* 1994, **372:**777-779
13. Merino JJ, Cordero MI and Sandi C **Regulation of hippocampal cell adhesion molecules NCAM and L1 by contextual fear conditioning is dependent upon time and stressor intensity** *Eur J Neurosci* 2000, **12:**3283-3290
14. Fallon J and Longhlin S **Substantia nigra** *The rat nervous system (Edited by: Paxinos G) San Diego: Academic Press* 1995, 215-238
15. Sakanaka M, Shiosaka S, Takatsuki K, Inagaki S, Takagi H, Senba E, Kawai Y, Matsuzaki T and Tohyama M **Experimental immunohistochemical studies on the amygdalofugal peptidergic (substance P and somatostatin) fibers in the stria terminalis of the rat** *Brain Res* 1981, **221:**231-242
16. Miragall F, Kadmon G, Husmann M and Schachner M **Expression of cell adhesion molecules in the olfactory system of the adult mouse: presence of the embryonic form of N-CAM** *Dev Biol* 1988, **129:**516-531

17. Lyckman AW, Moya KL, Confaloni A and Jhaveri S **Early postnatal expression of L1 by retinal fibers in the optic tract and synaptic targets of the Syrian hamster** *J Comp Neurol* 2000, **423:**40-51
18. Tsuru A, Mizuguchi M, Uyemura K and Takashima S **Immunohistochemical expression of cell adhesion molecule L1 during development of the human brain** *Early Hum Dev* 1996, **45:**93-101
19. Sandi C, Merino JJ, Cordero MI, Touyarot K and Venero C **Effects of chronic stress on contextual fear conditioning and the hippocampal expression of the neural cell adhesion molecule, its polysialylation, and L1** *Neuroscience* 2001, **102:**329-339
20. Becker CG, Becker T and Meyer RL **Increased NCAM-180 immunoreactivity and maintenance of L1 immunoreactivity in injured optic fibers of adult mice** *Exp Neurol* 2001, **169:**438-448
21. Hulley P, Schachner M and Lubbert H **L1 neural cell adhesion molecule is a survival factor for fetal dopaminergic neurons** *J Neurosci Res* 1998, **53:**129-134
22. Aubert I, Ridet JL, Schachner M, Rougon G and Gage FH **Expression of L1 and PSA during sprouting and regeneration in the adult hippocampal formation** *J Comp Neurol* 1998, **399:**1-19
23. Weiler IJ and Greenough WT **Potassium ion stimulation triggers protein translation in synaptoneurosomal polyribosomes** *Mol Cell Neurosci* 1991, **2:**305-314
24. Sidman RL, Angevine JB and Pierce ET *Atlas of the mouse brain and spinal cord Cambridge: Harverd University Press* 1971,
25. Hof PR, Young WG, Bloom FE, Belichenko PV and Celio MR *Comparative cytoarchitectonic atlas of the C57BL/6 and 129/Sv mouse brains Amsterdam: Elsevier* 2000,